

Activationless dynamic solvent effect

Serguei Feskov ^a, Vladislav Gladkikh ^b, Anatoly I. Burshtein ^{b,*}

^a Department of Physics, Volgograd State University, University Avenue, 100, Volgograd 400062, Russia

^b Weizmann Institute of Science, Rehovot 76100, Israel

Received 15 June 2007; in final form 30 August 2007

Available online 6 September 2007

Abstract

The dynamic solvent effect (DSE) is studied numerically at any free energy of electron transfer. In the activationless case the exact result known for an irreversible transfer is confirmed but the commonly accepted approximate results for reversible transfer were corrected. The general rate dependence on electron coupling is shown to fit the Zusman interpolation between the perturbation theory and DSE, not only in the normal and inverted region but in the activationless case as well. DSE is responsible for the saturation of the electron transfer at short distances where the electron coupling becomes strong.

© 2007 Published by Elsevier B.V.

1. Introduction

The electron transfer between the molecules separated by distance r is mainly determined by the electron coupling between the donor and acceptor parabolic terms, V . Since the tunnelling length L is short compared to the contact distance σ , the coupling

$$V = V_0 e^{-2(r-\sigma)/L}, \quad (1.1)$$

sharply decreases with inter-particle separation. At relatively long r it is rather small and the perturbation theory quadratic in coupling leads to the famous Marcus rate of electron transfer [1]:

$$W_{\text{PT}}(r) = \frac{V^2}{\hbar} \frac{\sqrt{\pi}}{\sqrt{\lambda T}} \exp\left(-\frac{(\Delta G + \lambda)^2}{4\lambda T}\right), \quad (1.2)$$

where ΔG is the free energy and λ is the reorganization energy of electron transfer ($k_B = 1$).

At shorter distances the coupling becomes too large and the weak non-adiabatic transfer gives way to a strong one [2]. The latter known as the dynamical solvent effect (DSE) can be also considered as adiabatic passage over a cusped barrier separating the wells. The transition from the weak

to strong non-adiabatic transfer is given by the general Zusman interpolation derived for highly activated transfer [3,4]:

$$W_Z = \frac{W_{\text{PT}}}{1 + W_{\text{PT}}/W_{\text{DSE}}} = \begin{cases} W_{\text{PT}} & \text{at } V \rightarrow 0, \\ W_{\text{DSE}} & \text{at } V \rightarrow \infty. \end{cases} \quad (1.3)$$

The DSE rate

$$W_{\text{DSE}} = \frac{1}{\tau} \exp\left(-\frac{(\Delta G + \lambda)^2}{4\lambda T}\right) \quad (1.4)$$

is inverse in τ which is the time of reaching the crossing point by diffusional motion along the reaction coordinate. The latter is proportional to τ_L which is the longitudinal relaxation time of polar solvent assisting the transfer. For highly activated transfer in either the normal ($-\Delta G < \lambda$) or inverted Marcus region ($-\Delta G > \lambda$) there is the following relationship between these times established by Zusman [3]:

$$\frac{1}{\tau} = \frac{1}{\tau_L \sqrt{4\pi\lambda T}} \frac{|\Delta G + \lambda||\Delta G - \lambda|}{|\Delta G + \lambda| + |\Delta G - \lambda|}. \quad (1.5)$$

The resonant transfer ($\Delta G = 0$) is really highly activated when its activation energy $\lambda/4 \gg T$. According to the Zusman formula (1.5) its rate is

$$\frac{1}{\tau_0} = \frac{1}{4\tau_L} \sqrt{\frac{\lambda}{\pi T}}. \quad (1.6)$$

* Corresponding author. Fax: +972 89344123.

E-mail address: cfbursh@wisemail.weizmann.ac.il (A.I. Burshtein).

A more general and accurate result (valid also for the lower friction and parabolic barrier) was derived later by Calef and Wolynes [5]. Applied to the highest friction and cusp barrier it takes the simplest form [6]:

$$\frac{1}{\tau} = \frac{1}{\tau_0 J_0(\lambda)} \quad \text{at } \Delta G = 0, \quad (1.7)$$

which is identical to the Zusman Eq. (1.6) provided $J_0(\lambda) = 1$. What actually happens is that [6]

$$J_0(\lambda) = -i\sqrt{\frac{\pi\lambda}{4T}} e^{-\lambda/4T} \text{erf}(i\sqrt{\lambda/4T}) \\ \approx 1 + \frac{2T}{\lambda} + 3\left(\frac{2T}{\lambda}\right)^2 + \dots \quad (1.8)$$

turns to 1 only when $\lambda/T \rightarrow \infty$.

Even at high λ the Zusman expression (1.5) is a reasonable approximation only in the normal and inverted Marcus regions where the transfer is highly activated, but completely incorrect in between, at $-\Delta G = \lambda$, where the transfer is activationless (Fig. 1). This particular case was investigated by Burshtein and Kofman [7] earlier than all others assuming that the transfer products are very unstable, so unstable that the reverse electron transfer from them to reactants is negligible. When diffusion to the crossing point is a limiting stage, the dissipation of initial state population was shown to be [7]

$$N = 2\pi^{-1} \arcsin e^{-t/\tau_L} \rightarrow 2\pi^{-1} e^{-t/\tau_L} \quad \text{at } t \gg \tau_L. \quad (1.9)$$

Hence the rate of the long time asymptotic decay of such an irreversible activationless transfer was found to be:

$$\frac{1}{\tau} = \frac{1}{\tau_L} \quad \text{at } -\Delta G = \lambda. \quad (1.10)$$

The non-exponential decay law (1.9) was then confirmed a number of times and even used to introduce the effective rate of transfer $k_d = \int_0^\infty N(t) dt = \frac{1}{\tau_L \ln 2}$ [8] which differs from the asymptotic value of the transfer rate (1.10). Nonetheless we restrict our discussion to only this parameter, $1/\tau(\Delta G)$.

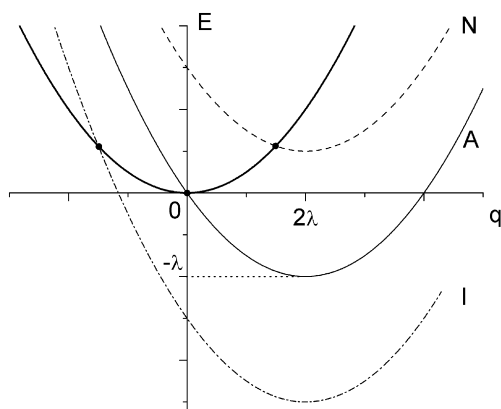


Fig. 1. The thermally activated electron transfer from the donor well (thick line) in either the normal region (to the well shown by the dashed line) or inverted region (to the well shown by the dash-dotted line) and the activationless transfer (to the well shown by the solid thin line A).

The limitations of the electron transfer activation and irreversibility were overcome by Rips and Jortner that made an attempt to find the true $\tau(\Delta G)$ dependence valid at any ΔG and λ [9]. As follows from their general Eq. (3.4) for the rate for the reversible activationless transfer,

$$\frac{1}{\tau} = \frac{1}{\tau_L} \frac{1}{\sqrt{\pi T/\lambda} + \ln 2} \rightarrow \frac{1}{\tau_L \ln 2} \quad (1.11)$$

as $\lambda \rightarrow \infty$, making the reverse transfer negligible. Since there is an odd factor $\ln 2$ compared to exact solution (1.10) for irreversible transfer, the rest of the results become also questionable and have to be inspected.

With this object in view, we will solve the problem numerically in the next section calculating the reversible electron transfer rate at any ΔG . In Section 3 we will specify the free energy dependence of $1/\tau$ and use it for getting W_{DSE} as well as W_Z . Obtained with the Zusman interpolation, the latter will be confirmed with the straightforward numerical calculation of the transfer rate at any ΔG and different couplings. In Section 4 the rate dependence on electron coupling will be visualized for the normal, activationless and inverted regions. We will also indicate the limitations of the theory due to the adiabatic cut off of electron transfer at the largest coupling.

2. Dynamic solvent effect

The general set of equations for the densities of reactants and products, $n_1(q, t)$ and $n_2(q, t)$, takes the following form [3,9]:

$$\dot{n}_1 = -a\delta(q - q^\dagger)[n_1 - n_2] + \frac{1}{\tau_L} \left[1 + q \frac{\partial}{\partial q} + \Delta^2 \frac{\partial^2}{\partial q^2} \right] n_1 \quad (2.1a)$$

$$\dot{n}_2 = a\delta(q - q^\dagger)[n_1 - n_2] + \frac{1}{\tau_L} \left[1 + (q - 2\lambda) \frac{\partial}{\partial q} + \Delta^2 \frac{\partial^2}{\partial q^2} \right] n_2, \quad (2.1b)$$

where

$$a = 2\pi V^2/\hbar, \quad \Delta = \sqrt{2\lambda T}$$

and the transfer is assumed to be located at the crossing point $q = q^\dagger$. This is the commonly accepted rate description of the population transfer between two energy levels started from 1980 [4,10]. To the activationless transfer the rate Eq. (2.1a) were applied even earlier being derived from the general density matrix equations (see Appendix to Ref. [7]).

In solving Eq. (2.1a) an assumption of initial thermal equilibrium in donor state is usually invoked while the product state is empty:

$$n_1(0) = \frac{\exp(-q^2/2\Delta^2)}{\sqrt{2\pi\Delta^2}}, \quad n_2(0) = 0. \quad (2.2)$$

As a matter of fact, the initial distribution is not ever thermal and the start is taken not necessarily from the bottom

of the well but this is a separate problem that will be considered elsewhere.

The general Eqs. (2.1) were solved numerically using the following technique. Let $G_1(q, t|q_0)$ and $G_2(q, t|q_0)$ be the Green functions for Eqs. (2.1) in the absence of electronic transitions ($V = a = 0$) when these equations take the form:

$$\left(\frac{\partial}{\partial t} - \hat{L}_k\right) G_k(q, t|q_0) = 0 \quad (k = 1, 2), \quad (2.3)$$

where \hat{L}_k are the operators of the free diffusion in the corresponding well. They should be solved with the initial conditions $G_k(q, t = 0|q_0) = \delta(q - q_0)$. The explicit form of these functions for the case of the parabolic wells is known to be

$$G_k(q, t|q_0) = \frac{1}{\sqrt{2\pi\Delta^2(t)}} \times \exp\left(-\frac{[q - q_k^{\min} - (q_0 - q_k^{\min})e^{-t/\tau_L}]^2}{2\Delta^2(t)}\right). \quad (2.4)$$

Here $\Delta^2(t) = \Delta^2(1 - e^{-2t/\tau_L})$, and $q_1^{\min} = 0, q_2^{\min} = 2\lambda$ are the potential minima positions in the reactant and product wells, correspondingly.

When $V \neq 0$, the set of the coupled Eqs. (2.1) has to be solved assuming that initially the system is localized at point q_0 on one or another term ($k_0 = 1, 2$). Such a solution can be presented as a vector, composed from the corresponding Green functions, $\bar{g}_{k_0}(q, t|q_0)$:

$$\bar{g}_{k_0}(q, t|q_0) = \begin{pmatrix} g_{1,k_0}(q, t|q_0) \\ g_{2,k_0}(q, t|q_0) \end{pmatrix}, \quad \bar{g}_{k_0}(q, t = 0|q_0) = \begin{pmatrix} \delta(q - q_0)\delta_{1,k_0} \\ \delta(q - q_0)\delta_{2,k_0} \end{pmatrix}, \quad (2.5)$$

where $\delta_{i,j}$ is the Kronecker symbol. The components of this vector obey the integral equations

$$\begin{aligned} g_{1,k_0}(q, t|q_0) &= \delta_{1,k_0} G_1(q, t|q_0) - \int dt' \int dq' K_{k_0}(q', t') \\ &\quad \delta(q' - q^\dagger) G_1(q, t - t'|q'), \\ g_{2,k_0}(q, t|q_0) &= \delta_{2,k_0} G_2(q, t|q_0) + \int dt' \int dq' K_{k_0}(q', t') \\ &\quad \delta(q' - q^\dagger) G_2(q, t - t'|q'), \end{aligned} \quad (2.6)$$

whose kernel is $K_{k_0}(q, t) = a(g_{1,k_0} - g_{2,k_0})$. The integration of Eq. (2.6) over q' yields

$$\begin{aligned} g_{1,k_0}(q, t|q_0) &= \delta_{1,k_0} G_1(q, t|q_0) \\ &\quad - \int dt' K_{k_0}(q^\dagger, t') G_1(q, t - t'|q^\dagger), \\ g_{2,k_0}(q, t|q_0) &= \delta_{2,k_0} G_2(q, t|q_0) \\ &\quad + \int dt' K_{k_0}(q^\dagger, t') G_2(q, t - t'|q^\dagger). \end{aligned} \quad (2.7)$$

Taking the Laplace transformation of these equations

$$\begin{aligned} \tilde{g}_{1,k_0}(q, s|q_0) &= \delta_{1,k_0} \tilde{G}_1(q, s|q_0) - \tilde{K}_{k_0}(q^\dagger, s) \tilde{G}_1(q, s|q^\dagger), \\ \tilde{g}_{2,k_0}(q, s|q_0) &= \delta_{2,k_0} \tilde{G}_2(q, s|q_0) + \tilde{K}_{k_0}(q^\dagger, s) \tilde{G}_2(q, s|q^\dagger), \end{aligned} \quad (2.8)$$

and substituting them into the definition of $\tilde{K}_{k_0}(q, s)$, we can resolve the equation obtained regarding $\tilde{K}_{k_0}(q^\dagger, s)$:

$$\tilde{K}_{k_0}(q^\dagger, s) = \frac{\delta_{1,k_0} a \tilde{G}_1(q^\dagger, s|q_0) - \delta_{2,k_0} a \tilde{G}_2(q^\dagger, s|q_0)}{1 + a[\tilde{G}_1(q^\dagger, s|q^\dagger) + \tilde{G}_2(q^\dagger, s|q^\dagger)]}. \quad (2.9)$$

Using the last result in Eq. (2.8), we can now proceed further making inverse Laplace transformation of them and getting the vector $\bar{g}_{k_0}(q, t|q_0)$ from Eq. (2.5). This can be done numerically using several different computational techniques (see, e.g. [11, 12]). We however found that the Euler summation scheme [13] of Abate and Whitt gives probably the best compromise between the precision and efficiency of the numerical calculations.

In principle, having known the Green function (2.5), one can directly calculate the densities of particles in each well at any time t as an integral over their initial distributions

$$n_k(q, t) = \int dq' [n_1(q', 0) g_{k,1}(q, t|q') + n_2(q', 0) g_{k,2}(q, t|q')]. \quad (2.10)$$

The difficulty here is the numerical evaluation of the Laplace transformation $\tilde{G}(q, s|q_0)$, which presents a computational problem. This difficulty can be avoided with the following minor modification of the algorithm. Let us introduce a grid of N points q_i on the reaction coordinate axis and denote $\Omega_{lk}(q_j|q_i) = g_{l,k}(q_j, \Delta t|q_i)$. Then, the probability to fall inside the $[q_j, q_{j+1}]$ interval on the l th electronic term, for the particle being initially at q_i on the k th term, by the time Δt is approximated by $\Omega_{lk}(q_j|q_i)\Delta q_j$. Here $\Delta q_j = q_{j+1} - q_j$ is the mesh width of the grid. If the time step Δt is small ($\Delta t \ll \tau_L$), the parabolic potentials near the q_i point can be replaced by straight lines with the slopes $A_1 = q_i/2\lambda$ and $A_2 = q_i/2\lambda - 1$. After such a linearization the Laplace transformation of the Green function, $\tilde{G}_k^{\text{lin}}(q, s|q_0)$, can be obtained in the close analytic form

$$\begin{aligned} \tilde{G}_k^{\text{lin}}(q, s|q_0) &= \frac{\tau_L}{\sqrt{a_k^2 + 4bs}} \\ &\quad \times \exp\left(-\frac{a_k}{2b}(q - q_0) - \frac{\sqrt{a_k^2 + 4bs}}{2b}|q - q_0|\right), \end{aligned} \quad (2.11)$$

$$a_k = \frac{2\lambda}{\tau_L} A_k, \quad b = \frac{\Delta^2}{\tau_L}.$$

Using $\tilde{G}_k^{\text{lin}}(q, s|q_0)$ instead of $\tilde{G}_k(q, s|q_0)$ in Eqs. (2.8) and (2.9), and the Abate–Whitt method for the numerical Laplace inversion, we calculated the quantities $\Omega_{lk}(q_j|q_i)$ for the fixed time interval Δt . Then replacing the integration

in Eq. (2.10) by summation, we obtained the following simple computational scheme:

$$\begin{aligned} n_1(q_i, t + \Delta t) &= \sum_j \Delta q_j [\Omega_{11}(q_i|q_j)n_1(q_j, t) + \Omega_{12}(q_i|q_j)n_2(q_j, t)], \\ n_2(q_i, t + \Delta t) &= \sum_j \Delta q_j [\Omega_{21}(q_i|q_j)n_1(q_j, t) + \Omega_{22}(q_i|q_j)n_2(q_j, t)]. \end{aligned} \quad (2.12)$$

We tested this algorithm in some limiting cases. Good agreement between the numerical and analytic results was found. The QM2L simulation software is available on the Internet (<http://physics.volsu.ru/feskov/software.htm>).

Let's follow the time evolution of the total populations in two wells,

$$N(t) = \int n_1(q, t) dq, \quad M(t) = \int n_2(q, t) dq, \quad (2.13)$$

approaching over time the equilibrium values $N_s = N(\infty)$ and $M_s = M(\infty)$. We are mainly concerned with highly exothermic transfer, when

$$N_s \ll M_s \approx 1 \quad \text{since} \quad -\Delta G \gg T. \quad (2.14)$$

Setting $N_s = 0$ one can expect that in such a situation equilibration proceeds exponentially at long times:

$$N(t) = 1 - M(t) \simeq e^{-Wt} \quad \text{at} \quad t \rightarrow \infty. \quad (2.15)$$

Obtained as an approximate solution of Eq. (2.1), $N(t)$ provides us with information about the magnitude and the free energy dependence of the transfer rate $W(\Delta G)$.

3. Zusman rate

As follows from the Zusman interpolation (1.3), W_Z approaches its maximum, when the coupling increases:

$$W_Z \rightarrow W_{DSE} = \frac{1}{\tau} \exp\left(-\frac{(\Delta G + \lambda)^2}{4\lambda T}\right) \quad \text{at} \quad V \rightarrow \infty. \quad (3.1)$$

Taking rather large V we calculated numerically the dynamic solvent effect rate as well as τ which is different at different ΔG . The free energy dependence $1/\tau(\Delta G)$ is shown in Fig. 2. It looks similar to that presented in Fig. 1 of Rips and Jortner's work [9] where the ratio $\tau(0)/\tau(\Delta G)$ is plotted versus ΔG . However, there is a significant difference between these two presentations. As seen from our Fig. 2, the absolute value $1/\tau$ obtained numerically differs from that given by the analytic Zusman approximation (1.5) even at $(\Delta G + \lambda)^2 \gg 4\lambda T$ where the latter is valid. This difference is masked when the ratio $\tau(0)/\tau(\Delta G)$ is considered instead of $1/\tau(\Delta G)$. For instance at resonant transfer ($\Delta G = 0$) the difference in absolute values of $1/\tau$ is about 5%, while the relative values are indistinguishable being both equal to 1.

This difference is worthy of special attention. The resonant transfer is out of the region (2.14) where the reaction is highly exergonic and therefore irreversible. In case of resonance the potential wells after equilibration are equipopulated,

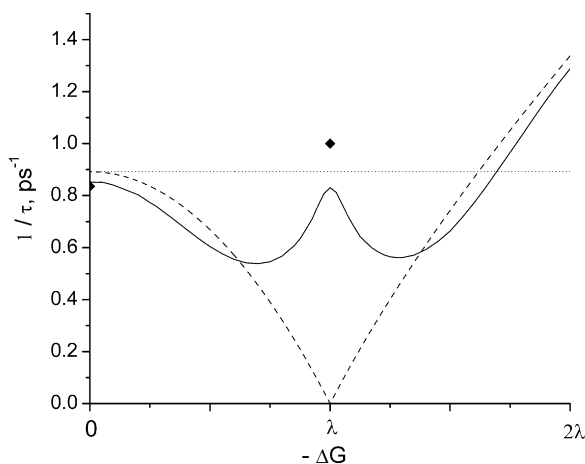


Fig. 2. The free energy dependence of the inverse τ calculated numerically at $\lambda = 1$ eV (solid line) and approximated by the Zusman analytical expression (1.5) (dashed line) and by the Calef–Wolynes estimate of the resonance transfer pre-exponent (1.7), shown by the triangle on the ordinate axis. The Burshtein–Kofman result for the irreversible activationless transfer (at $-\Delta G = \lambda$) is shown by the square point above the maximum.

$$N_s = M_s = 1/2 \quad \text{at} \quad \Delta G = 0 \quad (3.2)$$

and the system approaches this distribution non-exponentially. However, within certain time limits at the very beginning, the equilibration kinetics develops linearly in time allowing to specify W :

$$N = \frac{1}{2} [1 + e^{-2Wt}] \approx 1 - Wt \quad \text{at} \quad Wt \ll 1. \quad (3.3)$$

A completely different type of situation occurs in the case of activationless transfer ($\Delta G + \lambda = 0$) to which the Zusman approximation (1.5) is inapplicable. In this approximation $W = 1/\tau = 0$ contrary to the Burshtein–Kofman prognosis (1.10) given for an activationless irreversible transfer: $\tau = \tau_L$. For the reversible transfer of this sort the result is different but also finite as follows from the Rips–Jortner estimate (1.11). However, this expression is questionable because it does not reduce to its irreversible analog (1.9). As seen from Eq. (2.1b) the flux from the crossing point to the bottom of the product well is proportional to $2\lambda/\tau_L$. In the vicinity of the crossing point this well should be completely exhausted when $\lambda \rightarrow \infty$ ($\lim_{\lambda \rightarrow \infty} n_2(0) = 0$) so that the reverse transfer is excluded. The rate of irreversible transfer is the greatest possible. At our $\lambda = 1$ eV it exceeds the maximal $1/\tau$ for reversible transfer (calculated numerically) by 17%.

Although expression (1.11) overestimates the upper limit for the transfer rate its functional form is reasonable. Being represented as a linear relationship,

$$\frac{\tau}{\tau_L} = \alpha \sqrt{\pi T/\lambda} + \beta, \quad (3.4)$$

it was inspected numerically. The linearity was confirmed (Fig. 3) but the tangent α is 0.7 instead of 1 expected in

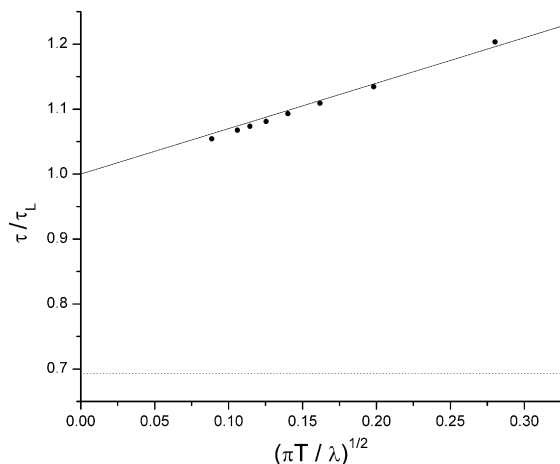


Fig. 3. Approaching the irreversible transfer limit, $\lim_{\lambda \rightarrow \infty} \tau/\tau_L = 1$. The points are the numerical results interpolated by a straight line. The dotted line indicates $\tau/\tau_L = \ln 2$.

(1.11) and $\beta = 1$ instead of $\ln 2$. The numerical results confirm the identity (1.10) which is an upper limit for the maximal τ reached at the largest λ (square point in Fig. 2).

For the simplest approximate estimation of $1/\tau$ it was recommended in Ref. [9] to set it equal to the Zusman value for resonant transfer, $1/\tau_0$. This average value shown by the dotted line in Fig. 2, differs from the real ones by not more than 40%. Being used in Eq. (1.4) for approximate estimation of W_{DSE} , it leads to the following universal formula for the Zusman rate:

$$W_Z \approx \frac{W_{\text{PT}}}{1 + \frac{V^2}{h} \frac{\sqrt{\pi}}{\sqrt{\lambda T}} \tau_0} = \frac{\frac{V^2}{h} \frac{\sqrt{\pi}}{\sqrt{\lambda T}}}{1 + \frac{4\pi V^2}{h\lambda} \tau_L} \exp\left(-\frac{(\Delta G + \lambda)^2}{4\lambda T}\right). \quad (3.5)$$

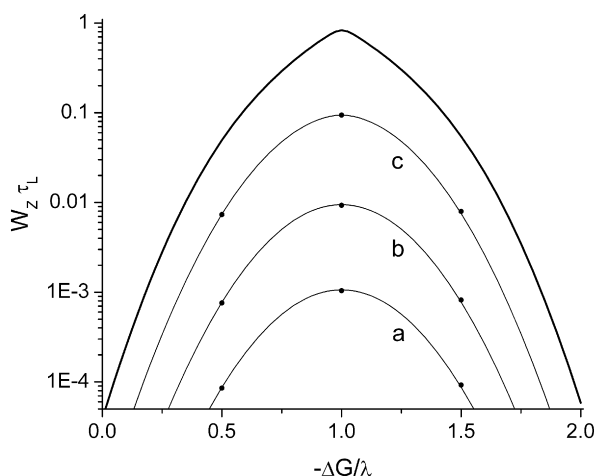


Fig. 4. The electron transfer rates obtained with the Zusman interpolation (1.3) using the numerically calculated DSE rate (upper thick line) and perturbation theory for different couplings: $V_0 = 2.5 \times 10^{-4}$ eV (a); $V_0 = 7.5 \times 10^{-3}$ eV (b); $V_0 = 2.5 \times 10^{-3}$ eV (c). The points are the same rates but numerically calculated for some free energies.

This approximation was used in Ref. [14] to specify the rates of two parallel electron transfer channels: quasi-resonant and highly exothermic.

Having numerically obtained solid data for $1/\tau$ we were now ready to make the calculations of the rate at any electron coupling. Using the exact estimation of W_{DSE} from Eq. (1.4) along with W_{PT} from Eq. (1.2), we obtained the Zusman transfer rates (1.3) for a few different electron couplings (Fig. 4). The results were confirmed by the straightforward numerical calculations of a few points in the normal, activationless and inverted regions. This is a convincing demonstration that the Zusman interpolation (1.3) is valid everywhere, even in the activationless case to which his estimation of τ , Eq. (1.4), is inapplicable.

4. The rate dependence on electron coupling

In any vertical cross-section of Fig. 4 at a given ΔG , we obtain the rate dependence on coupling V , which is quadratic in V until the perturbation theory holds but finally saturates approaching the DSE limit. In Fig. 5 we demonstrate the transfer rate saturation with V in three different cross-sections: normal, activationless and inverted. Everywhere the linearity of $\ln W$ in $\ln V$ (with a slope 2) indicates the region where the perturbation theory is valid, while the horizontal plateau represents the dynamic solvent effect.

As a matter of fact, this plateau gives way to the Kramers adiabatic cut off at even larger V . This effect was studied separately for the resonant transfer [6] and highly exergonic transfer in the inverted region [15]. In both cases there are the limitations of the Zusman interpolation separating it from the highest coupling (Kramers) limit. In the case of resonant transfer it follows from Eq. (2.7) of Ref. [6]:

$$V \ll 2\pi T J_0^2(\lambda) < 2\pi T. \quad (4.1)$$

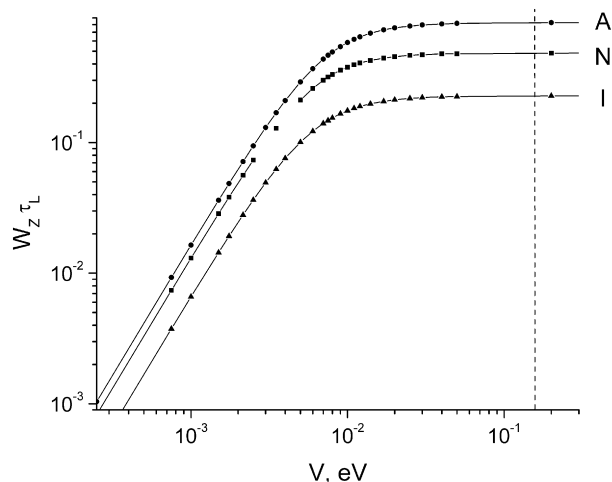


Fig. 5. The electron coupling dependence of the Zusman transfer rate in the activationless case A ($|\Delta G| = \lambda = 1$ eV), normal region, N ($|\Delta G|/\lambda = 0.85$), inverted region, I ($|\Delta G|/\lambda = 1.3$). All the points were numerically calculated.

Such an upper boundary for V is shown by the vertical dashed line in Fig. 5. In fact, it confines the present theory to the situation where the splitting in the crossing point is less than the thermal energy. At very small $\lambda \sim 0.2 - 0.5$ eV there is also one more limitation: the splitting should be smaller than the barrier which is $\lambda/4$ at resonance transfer. At larger coupling the barrier disappears and the exciplexes are formed [16–18].

5. Conclusions

As seen from Eq. (1.1) the coupling changes exponentially with inter-particle separation, reaching the maximal value at the closest approach distance. If this value, V_0 , is low enough the DSE plateau is not reachable and the perturbation theory result, Eq. (1.2), holds at any r . This is the commonly used approximation for weak transfer [1,19]. If the coupling turns out to be strong at short distances, the Zusman interpolation (1.3) should be used instead as in Ref. [14] (see Figs. 1 and 2). Here we proved that this interpolation accounts well for the DSE at any ΔG , provided τ is correctly estimated, either analytically or numerically.

Acknowledgements

FSV gratefully acknowledges the Weizmann Institute of Science for the hospitality during his stay in Israel, and the

Russian Foundation for Basic Research for support (Grants Nos. 04-03-95502 and 05-03-32680).

References

- [1] A.I. Burshtein, Adv. Chem. Phys. 114 (2000) 419.
- [2] B.I. Yakobson, A.I. Burshtein, High. Energy. Chem. 14 (1981) 211 [KhVE 14 (1980) 291].
- [3] L.D. Zusman, Zeit. Phys. Chem. 186 (1994) 1.
- [4] L.D. Zusman, Chem. Phys. 49 (1980) 295.
- [5] D.F. Calef, P.G. Wolynes, J. Phys. Chem. 87 (1983) 3387.
- [6] V. Gladkikh, A.I. Burshtein, I. Rips, J. Phys. Chem. A 109 (2005) 4983.
- [7] A.I. Burshtein, A.G. Kofman, Chem. Phys. 40 (1979) 289.
- [8] D.J. Bicout, A. Szabo, J. Chem. Phys. 109 (1998) 2325.
- [9] I. Rips, J. Jortner, J. Chem. Phys. 87 (1987) 6513.
- [10] B.I. Yakobson, A.I. Burshtein, Chem. Phys. 49 (1980) 385.
- [11] W.T. Weeks, J. ACM 13 (1966) 419.
- [12] B. Davies, B. Martin, J. Comput. Phys. 33 (1979) 1.
- [13] J. Abate, W. Whitt, ORSA J. Comput. 7 (1995) 36.
- [14] V. Gladkikh, G. Angulo, S. Pagés, B. Lang, E. Vauthey, J. Phys. Chem. A 108 (2004) 6667.
- [15] A.I. Burshtein, V. Gladkikh, Chem. Phys. 325 (2006) 359.
- [16] I.R. Gould, R.H. Yong, L.I. Mueller, S. Farid, J. Am. Chem. Soc. 116 (1994) 8176.
- [17] I.R. Gould, R.H. Yong, L.I. Mueller, L.C. Albrecht, S. Farid, J. Am. Chem. Soc. 116 (1994) 8188.
- [18] M.G. Kuzmin, I.v. Soboleva, E.V. Dolotova, High energy Chem. 40 (2000) 234.
- [19] A.I. Burshtein, Adv. Chem. Phys. 129 (2004) 105.